

Intrinsic Electrical and Thermal Properties from Single Crystals of $\text{Na}_{24}\text{Si}_{136}$

M. Beekman,¹ W. Schnelle,² H. Borrmann,² M. Baitinger,² Yu. Grin,^{2,†} and G. S. Nolas^{1,*}

¹*Department of Physics, University of South Florida, Tampa, Florida, USA*

²*Max-Planck-Institut für Chemische Physik fester Stoffe, Dresden, Germany*

(Received 17 September 2009; published 8 January 2010)

The observation of intrinsic structural, electrical, and thermal properties from measurements on single-crystal specimens of clathrate-II $\text{Na}_{24}\text{Si}_{136}$ is reported, revealing metallic conduction in agreement with electronic structure calculations. Low-temperature heat capacity measurements corroborate a substantial electronic density of states at the Fermi level, and reveal an Einstein-like mode that can be attributed to Na guest “rattling”. The large thermal conductivity of $\text{Na}_{24}\text{Si}_{136}$, compared to literature data for other intermetallic clathrates, can be understood in terms of the predominant electronic contribution for the fully filled $\text{Na}_{24}\text{Si}_{136}$ composition.

DOI: 10.1103/PhysRevLett.104.018301

PACS numbers: 82.75.-z, 65.40.Ba, 72.15.Eb

Because of formidable synthetic challenges, many materials of scientific and technological interest are first obtained as microcrystalline powders, and thus care must be taken in interpretation of the observed structural, chemical, and physical properties, which can be strongly influenced by grain boundary effects, surface composition, and impurity phases. A canonical example is the intermetallic clathrate-II system $\text{Na}_x\text{Si}_{136}$ ($0 \leq x \leq 24$) [1]. Characterized by a covalently bonded cagelike framework crystal structure isotypic to the H_{II} clathrate hydrate, this material system has stimulated much interest from both fundamental [2–4] and applied [2,5–8] vantage points. Yet in the four decades since the discovery [1] of this material, the preparation of single crystals was not achieved, and all investigations to date have utilized the available microcrystalline $\text{Na}_x\text{Si}_{136}$ specimens typically prepared by the previously established method of thermal decomposition of the Zintl compound Na_4Si_4 [1].

The electronic structure of the $\text{Na}_x\text{Si}_{136}$ clathrates has received considerable theoretical attention [2,5,7,9] in an effort to understand the influence of Na loading of the framework polyhedral cages on the electronic properties of this system. In particular, a reported metal-to-insulator transition with composition, i.e., the Na content x , in this system has been much discussed, with several proposed explanations [2,5,7,9,10]. Electrical properties have been inferred from measurements on microcrystalline samples [1,10–12], but achieving a fundamental understanding of the conduction in these materials, and their physical properties more generally, has remained elusive [2]. A key challenge lies in the interpretation of transport and other physical properties measurements which have been hindered and in some cases dominated by extrinsic effects originating in the microcrystalline nature of the specimens and associated difficulties in consolidation [1,10,12]. Here we have used a recently developed technique [13] to grow phase-pure, single-crystal clathrate-II $\text{Na}_{24}\text{Si}_{136}$ specimens for intrinsic physical properties determination. The preparation of phase-pure crystals is note-

worthy, since preparation of single-phase $\text{Na}_x\text{Si}_{136}$ specimens (in microcrystalline powder form from thermal decomposition) is challenging [14,15].

Heat capacity was measured on single-crystal specimens (2.349 mg mass) using a Quantum DesignTM Physical Properties Measurement System. Temperature dependent four-probe electrical resistivity, Seebeck coefficient, and steady-state thermal conductivity measurements were carried out in a custom closed-cycle helium cryostat [16]. The transport data were reproduced on several crystals. The temperature dependence showed excellent repeatability, and the magnitude agreed within the estimated relative uncertainty of $\sim 30\%$ associated with the determination of the geometrical factor for the crystals.

Single-crystal x-ray diffraction studies established [13] that all Na and Si crystallographic sites in the clathrate-II crystal structure are completely occupied, confirming the stoichiometric composition $\text{Na}_{24}\text{Si}_{136}$. An exceptionally large atomic displacement parameter (U_{eq}) obtained for Na ($8b$ site) in the Si_{28} cage (denoted hereafter as Na@Si_{28}) is suggestive of large amplitude thermal motion, or “rattling,” for this Na guest within its oversized Si_{28} cage. Assuming a harmonic oscillator model (representing an Einstein mode associated with the Na guest), an estimate of the vibrational frequency, ν , can be obtained [17] from the room temperature $U_{\text{eq}} = 0.110(2) \text{ \AA}^2$, and the relation $U_{\text{eq}} = k_B T / [m(2\pi\nu)^2]$. Here k_B is Boltzmann’s constant, m is the mass of the Na atom, and $T = 293 \text{ K}$. Applying this model, a characteristic Einstein temperature $\Theta_E = h\nu/k_B$, where h is Planck’s constant, of 75 K is inferred using U_{eq} for Na@Si_{28} when centered at the $8b$ site. Though this value of Θ_E is interpreted only as an estimate, it evidences the presence of a low-frequency phonon mode associated with the Na@Si_{28} guest.

An Einstein mode for Na@Si_{28} is more conclusively observed from the measured specific heat, where the presence of these entropic degrees of freedom is apparent. The measured specific heat $C_p(T)$ for $\text{Na}_{24}\text{Si}_{136}$ is shown in Fig. 1. Plotting the data as C_p/T^3 vs. T reveals clear

evidence of low energy Einstein mode contributions to the specific heat, which appear as a peak in the temperature dependence in this representation [18]. The Einstein mode contribution to C_p is also unequivocally apparent from the data when presented as C_p/T vs. T [inset to Fig. 1(b)]. Measurement of C_p in applied magnetic fields up to 9 T confirmed the peaked feature in C_p is independent of magnetic field. Considering the contributions to C_p that are expected to be significant in this temperature range [19], a model comprised of a linear combination of terms was fit to the data:

$$C_p(T) \approx C_v(T) = C_e(T) + C_{E1}(T) + C_{E2}(T) + C_D(T). \quad (1)$$

Here $C_e(T) = \gamma T$ is the electronic specific heat, γ is the Sommerfeld coefficient, and

$$C_{Ei}(T) = 3N_{Ei}R\left(\frac{\Theta_{Ei}}{T}\right)^2 \frac{\exp(\Theta_{Ei}/T)}{(\exp(\Theta_{Ei}/T) - 1)^2} \quad (2)$$

are Einstein oscillator contributions, where R is the gas constant, N_{Ei} and Θ_{Ei} are the number (per formula unit) and Einstein temperature of oscillator i , respectively. Two Einstein oscillator terms are included to account for the possibility of modes associated with the two different Na guests in the structure. The term

$$C_D(T) = 9N_D R \left(\frac{T}{\Theta_D}\right)^3 \int_0^{\Theta_D/T} \frac{x^4 e^x}{(e^x - 1)^2} dx \quad (3)$$

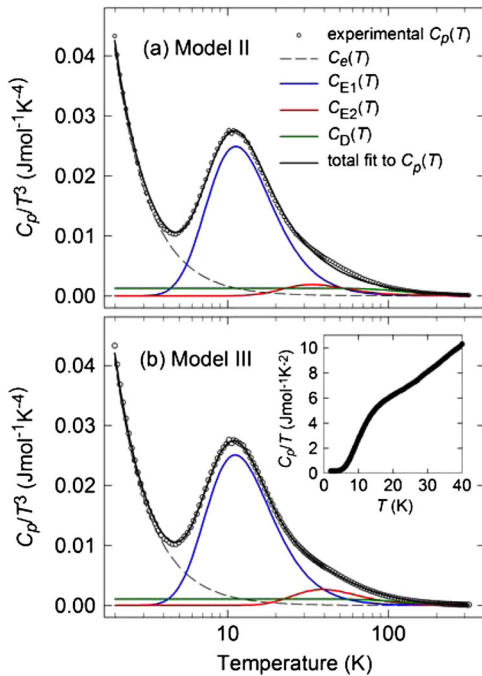


FIG. 1 (color online). Specific heat capacity of $\text{Na}_{24}\text{Si}_{136}$ plotted as C_p/T^3 against T , along with fits obtained with (a) Model II and (b) Model III described in Table I. Individual contributions to the overall fit are also shown as indicated. Inset to (b): The same experimental C_p data plotted as C_p/T against T , in the temperature range 0 to 40 K.

corresponds to the harmonic lattice specific heat in the Debye approximation, where $x = \hbar\omega/k_B T$, ω is the phonon angular frequency, N_D is the number of “Debye atoms” per formula unit, and Θ_D is the (temperature independent) Debye temperature. The value $\gamma = 0.163(4) \text{ J K}^{-2} \text{ mol}^{-1}$, determined from linear fits to C_p/T vs T^2 below 4 K, reflects a considerable electronic contribution to the specific heat and a substantial electronic density of states at the Fermi level typical of a metallic compound. This agrees with density functional calculations [7] for $\text{Na}_{24}\text{Si}_{136}$ which predict the Fermi level to coincide with a prominent peak in the electronic density of states, and also corroborates the metallic transport properties that are discussed below.

Fitting parameters corresponding to three different models are given in Table I, with the free parameters for each model indicated. For the fit in Fig. 1(a) (Model II), $N_{E1} = 8$, $N_{E2} = 16$, and $N_D = 136$, were assigned to correspond to $8 \times \text{Na@Si}_{28}$ and $16 \times \text{Na@Si}_{20}$ per formula unit, and the Si_{136} framework, respectively, and Θ_{E1} , Θ_{E2} , and Θ_D , were used as variable fitting parameters. It is evident from the fit that this simple model already describes the low-temperature $C_p(T)$ data very well. The Debye temperature of $\Theta_D = 593 \text{ K}$ corroborates $\Theta_D = 610 \text{ K}$ predicted [20] for the empty Si_{136} framework. The lowering of Θ_D is consistent with the increased Si-Si bond lengths and slightly weaker framework bonding for $\text{Na}_{24}\text{Si}_{136}$ [13] compared to Si_{136} [6]. The best fit, shown in Fig. 1(b), is achieved by allowing N_{E1} , N_{E2} , and N_D also to be free parameters, and results in a substantially higher weight of the higher energy Einstein mode (Table I). This likely reflects the inadequacy of the simple Debye model with a single temperature independent Θ_D to account for C_p over the entire temperature range, as well as the ability of the higher energy Einstein mode to more adequately model contributions to C_p at higher temperatures from the large number of optic modes in $\text{Na}_{24}\text{Si}_{136}$ resulting from the large number of atoms in the unit cell. The illuminating aspect to note is that when allowed as free parameters, the best fit values for N_{E1} and Θ_{E1} are $7.8 \approx 8$ and 55 K , respectively. The observations confirm the presence of a low energy Einstein-like mode clearly associated with the eight Na@Si_{28} guests per formula unit. The Θ_{E1} determined from specific heat data is lower than that obtained from U_{eq} above, which can also be affected by systematic errors such as absorption in the diffraction experiment. The clearly observed Einstein mode corroborates a large dynamic contribution to the disordered Na@Si_{28} . The frequency of this “rattle” mode falls well inside the frequency range of the host Si_{136} acoustic phonon branches predicted from density functional theory calculations [21] indicating the potential for a resonant phonon interaction, analogous to clathrate-I materials [22,23].

The magnetic susceptibility, $\chi(T)$, of $\text{Na}_{24}\text{Si}_{136}$ measured in an applied field of 3.5 T is shown in Fig. 2. Field-dependent measurements carried out in fields from

TABLE I. Values of parameters from fits to the $C_p(T)$ data shown in Fig. 1. Parameters that were held fixed for a particular model are denoted by *; parameters that were allowed to vary during least-squares fitting are denoted by †. Per formula unit, Model I corresponds to 152 Debye atoms (16Na + 136Si) and 8 (Na) Einstein oscillators, and Model II corresponds to 136 (Si) Debye atoms and 8 and 16 (Na) Einstein oscillators, respectively. Model III allows all parameters to be free parameters.

Model (free parameters)	γ (J mol ⁻¹ K ⁻²)	N_{E1}	Θ_{E1} (K)	N_{E2}	Θ_{E2} (K)	N_D	Θ_D (K)
I (Θ_{E1}, Θ_D)	0.16*	8*	56.3†	N/A	N/A	152*	506.3†
II ($\gamma, \Theta_{E1}, \Theta_D, \Theta_{E2}$)	0.16†	8*	55.5†	16*	165.5†	136*	593.4†
III ($\gamma, N_{E1}, \Theta_{E1}, N_{E2}, \Theta_{E2}, \Theta_{E2}, \Theta_D$)	0.16†	7.8†	54.9†	35.4†	192.1†	101.5†	575.0†

2 mT to 7 T and down to 2 K showed evidence of only very small contributions from paramagnetic or ferromagnetic impurities. The slight upturn in the data of Fig. 2 at the lowest temperatures can be attributed to the presence of trace paramagnetic impurities in the specimen originating in the starting silicon material or possibly introduced by tools used during specimen preparation. A relatively strong temperature dependence of $\chi(T)$ is observed, with both paramagnetic and diamagnetic regions. The increase and then decrease in $\chi(T)$ with decreasing temperature can be ascribed to a contribution $\chi_e(T)$ from the conduction electrons that is not temperature independent, suggesting sharp features in the electronic density of states near the Fermi level. Such peaked features in the density of states were observed in electronic structure calculations [7,24,25] and were invoked in order to explain the unusually strong temperature dependence of ²³Na Knight shifts observed from Na_xSi₁₃₆ powder specimens [24,25]. The Knight shifts (which are proportional to the Pauli susceptibility of the conduction electrons) previously observed from Na_xSi₁₃₆ showed a temperature dependence that is qualitatively very similar to $\chi(T)$ of Na₂₄Si₁₃₆ (Fig. 2), both exhibiting broad maxima just below 200 K [24,25].

Observation of intrinsic electronic transport in Na_xSi₁₃₆ clathrates has been previously obscured by extrinsic effects originating in the microcrystalline nature of the specimens [1,10,12]. As shown in Fig. 3(a), the temperature dependent electrical resistivity, $\rho(T)$, data for Na₂₄Si₁₃₆ reveal metallic conduction, with ρ for the crystal reaching the value 0.03 mΩ-cm at 300 K. The Seebeck coefficient, S [Fig. 3(a)], of Na₂₄Si₁₃₆ reaches the value $-5 \mu\text{V}/\text{K}$ at

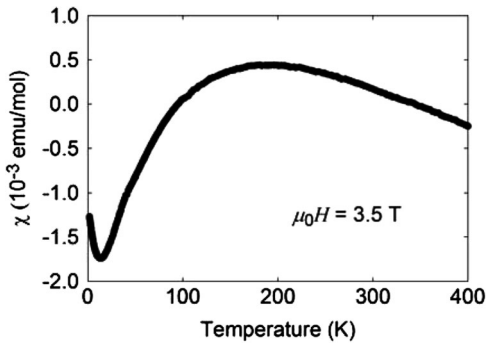


FIG. 2. Magnetic susceptibility of Na₂₄Si₁₃₆, measured in an applied field $\mu_0 H = 3.5$ T.

room temperature, consistent with a high density of electrons as the majority carriers and metallic conduction. Both simple crystal chemistry considerations and detailed density functional theory calculations [7,9] predict the location of the Fermi level to be well inside the conduction band for Na₂₄Si₁₃₆ with a high density of carriers expected. From the simple crystal chemistry formulation $[\text{Na}^+]_{24}[(4b)\text{Si}^0]_{136} \cdot 24e^-$ that assumes that each Na, being formally Na⁺, contributes one electron for conduction, and the room temperature unit cell volume of 3187 Å³, we can estimate an upper bound of $n = 7.5 \times 10^{21} \text{ cm}^{-3}$ for the room temperature carrier concentration of Na₂₄Si₁₃₆. Assuming $\rho = (ne\mu)^{-1}$ and a single carrier band, where e is the elementary charge, this implies a lower bound on the electron mobility of $\mu \sim 29 \text{ cm}^2 \text{ V}^{-1} \text{ s}^{-1}$, a relatively high value considering the high concentration of charge carriers. The inferred free electron relaxation time $\tau = m/\rho ne^2 = 1.6 \times 10^{-14} \text{ s}$, where m is the free electron mass, is comparable to room temperature values for the elemental alkali metals [26].

At the lowest temperature of our measurement (12 K), $d\rho/dT > 0$ indicating the residual resistivity for the specimen has still not yet been reached. Although a value for the

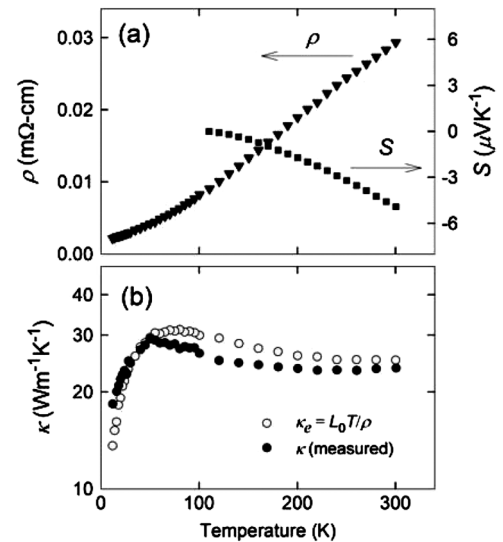


FIG. 3. (a) Electrical resistivity (ρ) and Seebeck coefficient (S) of Na₂₄Si₁₃₆. (b) Thermal conductivity (κ) of Na₂₄Si₁₃₆ (closed symbols) and calculated contribution (open symbols) estimated from the Wiedemann-Franz relation.

residual resistance ratio (RRR) incorporating data from lower temperatures will be larger, we calculate from our data a RRR of $\rho(300\text{ K})/\rho(12\text{ K}) = 14$. To our knowledge, this value is several times larger than the highest RRR values previously reported for known metallic clathrates (i.e., with $d\rho/dT$ positive definite), including both polycrystalline [27] and single-crystal clathrate-I specimens [28]. The relatively high RRR value for the $\text{Na}_{24}\text{Si}_{136}$ specimen, taken together with the above inferred mobility, is further indication of both the high quality of the crystal and the pronounced metallic conduction.

The thermal conductivity κ of $\text{Na}_{24}\text{Si}_{136}$, shown in Fig. 3(b), is relatively large in comparison to other intermetallic clathrates, which often exhibit very low and even glasslike thermal conductivities [22]. Indeed, the observed κ of $\text{Na}_{24}\text{Si}_{136}$ is substantially larger than previously observed for any intermetallic clathrate composition. Considering the pronounced metallic character observed in both C_p and ρ , a sizeable electronic contribution κ_e to the thermal conduction is expected. In a first approximation, employing the Wiedemann-Franz relation $\kappa_e = L_0 T / \rho$, a temperature independent Lorentz number $L_0 = 2.45 \times 10^{-8} \text{ V}^2 \text{ s}^{-2}$, and the measured electrical resistivity [Fig. 3(a)], an estimate of the electronic thermal conductivity κ_e can be calculated, and is plotted in Fig. 3(b) along with the experimentally measured thermal conductivity. Quantitative agreement is not expected [29], but the simple approximation nevertheless qualitatively captures the salient features of the experimental data in both magnitude and temperature dependence, indicating κ_e likely dominates κ . Obtaining a reliable estimate of the lattice thermal conductivity of a material such as $\text{Na}_{24}\text{Si}_{136}$ which contains such a large electronic contribution is nontrivial [29], but considering the low thermal conductivity of the empty Si_{136} framework [8], the presence of the low energy Einstein-like “rattle” mode clearly observed in the measured specific heat and discussed above, and the considerable expected [29] electron-phonon scattering in light of the high density of conduction electrons, it is reasonable to conclude that the lattice thermal conductivity of $\text{Na}_{24}\text{Si}_{136}$ is very low compared to the large κ_e component. Lattice thermal conductivities on the order of $2 \text{ W m}^{-1} \text{ K}^{-1}$ were estimated for the filled clathrate-II compositions $\text{Cs}_8\text{Na}_{16}\text{Si}_{136}$ and $\text{Rb}_8\text{Na}_{16}\text{Si}_{136}$ [30].

In summary, from physical properties measurements on single crystals of the fully filled clathrate-II $\text{Na}_{24}\text{Si}_{136}$, intrinsic transport and physical properties are observed experimentally for the first time. The data support density functional theory predictions and are also in agreement with simple crystal-chemical considerations. Conclusive experimental evidence of a low energy phonon mode associated with the $\text{Na}@\text{Si}_{28}$ guest atom is provided from the measured specific heat, while the thermal transport is dominated by the charge carriers. The $\text{Na}_{24}\text{Si}_{136}$ clathrate

constitutes an excellent model system for exploration of key physical concepts associated with structure-property relationships in intermetallic clathrate materials, which the availability of single crystals now allows.

M. Beekman and G. S. N. acknowledge support from US DOE Grant No. DE-FG02-04ER46145. M. Beekman also acknowledges support from DAAD. The authors thank K. Meier, R. Cardoso Gil, R. Koban, P. Scheppan, S. Müller, and A. Datta for their support and technical assistance.

*gnolas@cas.usf.edu

†grin@cpfs.mpg.de

- [1] J. S. Kasper *et al.*, *Science* **150**, 1713 (1965).
- [2] M. Beekman and G. S. Nolas, *J. Mater. Chem.* **18**, 842 (2008).
- [3] A. A. Demkov *et al.*, *Phys. Rev. B* **50**, 17001 (1994).
- [4] F. Brunet *et al.*, *Phys. Rev. B* **61**, 16550 (2000).
- [5] G. B. Adams *et al.*, *Phys. Rev. B* **49**, 8048 (1994).
- [6] J. Gryko *et al.*, *Phys. Rev. B* **62**, R7707 (2000).
- [7] J. C. Conesa, C. Tablero, and P. Wahnón, *J. Chem. Phys.* **120**, 6142 (2004).
- [8] G. S. Nolas *et al.*, *Appl. Phys. Lett.* **82**, 910 (2003).
- [9] V. I. Smelyansky and J. S. Tse, *Chem. Phys. Lett.* **264**, 459 (1997).
- [10] N. F. Mott, *J. Solid State Chem.* **6**, 348 (1973).
- [11] S. B. Roy, K. E. Sim, and A. D. Caplin, *Phil. Mag.* **65**, 1445 (1992).
- [12] M. Beekman and G. S. Nolas, *Physica B (Amsterdam)* **383**, 111 (2006).
- [13] M. Beekman *et al.*, *J. Am. Chem. Soc.* **131**, 9642 (2009).
- [14] G. K. Ramachandran *et al.*, *J. Solid State Chem.* **145**, 716 (1999).
- [15] E. Reny *et al.*, *J. Mater. Chem.* **8**, 2839 (1998).
- [16] J. Martin *et al.*, *J. Appl. Phys.* **99**, 044903 (2006).
- [17] J. D. Dunitz, V. Schomaker, and K. N. Trueblood, *J. Phys. Chem.* **92**, 856 (1988).
- [18] M. G. Alexander, D. P. Goshorn, and D. G. Onn, *Phys. Rev. B* **22**, 4535 (1980).
- [19] A. Tari, *The Specific Heat of Matter at Low Temperatures* (Imperial College Press, London, 2003).
- [20] K. Biswas *et al.*, *J. Appl. Phys.* **104**, 033535 (2008).
- [21] X. Tang *et al.*, *Phys. Rev. B* **74**, 014109 (2006).
- [22] J. L. Cohn *et al.*, *Phys. Rev. Lett.* **82**, 779 (1999).
- [23] G. S. Nolas *et al.*, *Phys. Rev. B* **61**, 3845 (2000).
- [24] J. Gryko *et al.*, *Phys. Rev. B* **57**, 4172 (1998).
- [25] J. He *et al.*, *J. Phys. Chem. B* **105**, 3475 (2001).
- [26] N. W. Ashcroft and N. D. Mermin, *Solid State Physics* (Saunders College Publishing, Orlando, 1976).
- [27] A. Bentien *et al.*, *Phys. Rev. B* **71**, 165206 (2005).
- [28] M. A. Avila *et al.*, *J. Phys. Condens. Matter* **18**, 1585 (2006).
- [29] R. Berman, *Thermal Conduction in Solids* (Oxford University Press, Oxford, 1976).
- [30] G. S. Nolas *et al.*, *J. Appl. Phys.* **91**, 8970 (2002).